Research Article

Tuning Rigid Polyurethane Foam with Eco-friendly Cellulose Nanocrystals from Oil Palm Empty Fruit Bunches as Energy-Efficient Material Composites for Buildings

Dilla Dayanti
Research Center for Environmental and Clean Technology, National Research and Innovation Agency, Bandung, Indonesia
Master Program of Energy, School of Postgraduate Studies, Diponegoro University, Semarang, Indonesia

Marcelinus Christwardana
Master Program of Energy, School of Postgraduate Studies, Diponegoro University, Semarang, Indonesia
Research Collaboration for Electrochemistry, BRIN-UNDIP, Indonesia

Nurlaili Fitria
Department of Chemistry, Faculty of Mathematics and Natural Sciences, Brawijaya University, Indonesia

Purwoko
Research Center for Aeronautics and Space, National Research and Innovation Agency, Bogor, Indonesia

Malinee Sriariyanun
Biorefinery and Process Automation Engineering Center, The Sirindhorn International Thai-German Graduate School of Engineering, King Mongkut's University of Technology North Bangkok, Bangkok, Thailand

Hidayat, Yohanes Susanto Ridwan and Sambas
Research Center for Environmental and Clean Technology, National Research and Innovation Agency, Bandung, Indonesia

Rushdan Ahmad Ilyas
Research Faculty of Chemical and Energy Engineering, Universiti Teknologi Malaysia, Johor, Malaysia

Pratheep Kumar Annamalai
Research School of Agriculture and Environmental Sciences, University of Southern Queensland, Toowoomba, Australia

Athanasia Amanda Septevani*
Research Center for Environmental and Clean Technology, National Research and Innovation Agency, Bandung, Indonesia
Research Collaboration for Nanocellulose, BRIN-Andalas University, Indonesia
Research Collaboration for Electrochemistry, BRIN-UNDIP, Indonesia

* Corresponding author. E-mail: atha001@brin.go.id DOI: 10.14416/j.asep.2024.09.001
Received: 6 June 2024; Revised: 10 July 2024; Accepted: 5 August 2024; Published online: 3 September 2024

Abstract
The development of novel materials based on renewable materials with beneficial properties that assist with energy efficiency and conservation has been encouraged by increasing consciousness of environmental issues. This research intends to use sustainable cellulose nanocrystals (CNC) obtained from oil palm empty fruit bunches (OPEFB) as reinforcement to enhance the properties of rigid polyurethane foam (RPUF). RPUF reinforcement with varied CNC concentrations (0.25–1 wt%) was examined by foaming behavior, surface morphology, mechanical properties, thermal insulation properties, dimensional stability, efficiency energy study, and CO_2 reduction through their thermal conductivity values. The results achieved an optimal improvement of mechanical properties of the RPUF composite by around 23.53% compared to RPUF control, at the addition of 0.5 wt% of CNC concentration while maintaining the density of 37–39 kg/m^3. Further, incorporating CNC improved thermal insulating performance by 9.95%, as reflected by decreased thermal conductivity from 0.0292 W/mK to 0.0269 W/mK and decreased cell size by 28.12%. Finally, based on the energy and cost efficiency studies, RPUF-CNC composites offer up to 0.78 kWh/m^2 and 0.031 kWh/m^2 compared to conventional wall materials made of concrete and wood, respectively. Furthermore, it contributed to reduced greenhouse gas (GHG) emissions by 110 and 7.2 kg CO_2/year compared to concrete and wood, respectively. This work demonstrates the promising use of eco-friendly building insulation materials to mitigate the energy and environmental crisis.

Keywords: Biocomposite, Cellulose nanocrystal, Energy-efficient, Rigid polyurethane foam, Thermal insulation

1 Introduction

Energy is an important aspect of mankind that mobilizes transportation and the economy of each country. As the population grows, the energy demand also increases, leading to an energy crisis that impacts the environment and society [1]. In 2018, building construction accounted for about 39% of carbon dioxide gas emissions, particularly in some developed countries, where rapid growth in building floor area led to an increase in building energy demand of more than 20% between 2000 and 2017. Heat transfer via building envelopes accounts for 60–80% of heating and cooling loads [2]. It has been demonstrated that enhancing the thermal performance of the building exterior can significantly increase the overall efficiency of the building in terms of energy consumption. The first step to achieving an energy-efficient building structure is by applying thermal insulation material to minimize the speed of heat transfer leading to a lower use of energy for air conditioners and heaters and thus saving energy [3].

Polyurethane foam, particularly at the rigid cell structure, is known as rigid polyurethane foam (RPUF) and has been recognized as a promising insulation material due to credible evidence of cost savings, heat reduction, radiation prevention, and durability characteristics that can be achieved at low-density within the range of 30–45 kg/m^3. Thermal conductivity is an important property of RPUF due to its primary use as a thermal insulation material. The sustainability of RPUF in terms of energy conservation is also dependent on the retention of thermal conductivity. The capacity to sustain low thermal conductivity over an extended period of time despite a rise in thermal conductivity as the material ages. Several studies have been carried out, such as making RPUF by adding reinforcing materials such as aluminum diethyl phosphinate [4], BP@MoS2 hydride [5], P/Cu-hybris silica aerogel (m-SA) [6], and graphene nanofiller [7] reinforcement to improve thermal and mechanical properties. However, the use of inorganic materials is expensive and environmentally unfriendly. Several recent studies reported that cellulose is one of the promising reinforcing materials in composite derived from renewable and eco-friendly to enhance mechanical properties and thermal insulation performance including coconut leaf stalk [8], bagasse [9], bamboo, and wood fiber [10]. A ball-milling process has been employed to synthesize composites of polyurethane with amorphous cellulose, resulting in a reduction of thermal conductivity to 33% [11]. The incorporation of natural fibers into polyurethane can improve its mechanical and thermal properties [12], [13]. The inclusion of nanocellulose reinforcement within a polyurethane matrix can enhance the dimensional stability of the nanocomposite [14]. In addition, the incorporation of hardwood porridge into a PU composite foam can increase cell size due to the presence of fibers [15].

As previously mentioned, cellulose has been recognized as a reinforcing filler that enhances mechanical and insulating properties. Cellulose is the

most abundant natural polymer, offering unique characteristics and benefits that enable its use in a wide range of applications, including composites, hydrogels, implants, filtration, packaging, paints, paper, and pulp. Cellulose can be derived from various sources, including wood, bacteria, annual plants, and algae. Besides cellulose, its derivatives are also widely explored in various fields [16]. Depending on the nature and local commodities, every country possesses abundantly available sources for cellulose production. Palm oil has been massively planted in Indonesia and Malaysia. Every 1 t production of palm oil will generate biomass waste in the form of oil palm empty fruit bunches (OPEFB) as much as 23% of which compose a high content of cellulose ranging from 23.7% to 65.0% [17]. Cellulose derived from OPEFB has been reported to be deconstructed further into nano-sized materials, in the form of Cellulose nanocrystals (CNCs). The typical CNC morphology has a diameter of 1–100 nm with an elongated shape of 500–2000 nm, offering a high surface area, low density, low coefficient of thermal expansion, low aspect ratio, and high specific strength. Because of these features, cellulose nanocrystals have attracted great attention over the past few years. The CNC from oil palm waste offers advantages because of its highest productivity over other crops and, high cellulose content compared to various resources of biomass, including rice straw [18], sugarcane bagasse [19], bamboo fibers [20], and walnut shell [21].

In recent research, several groups have investigated the use of CNC in the reinforcement of polyurethane (PU). The incorporation of 0.6 wt% of CNC into rigid polyurethane foam resulted in reduced thermal conductivity of up to 6% compared to control under room and cryogenic temperatures [22]. The effects of CNC from algae that could improve the compressive strength from 4.5 kPa to 4.7 kPa of rigid polyurethane were investigated by *Jonjaroen et. al.*, [23]. Redondo *et al*., [24] examined CNC derived from wood that could increase the compressive strength by 53.84% of rigid polyurethane. Furthermore, the incorporation of CNC from cotton into a segmented polyurethane foam matrix via effective dispersion could improve mechanical properties from 0.7 MPa to 1.3 MPa [25].

The incorporation of low-loading CNC has been reported to yield promising results for enhancing the thermal insulation performance of RPUF using renewable nanomaterials [26]. CNC has been known as promising nanofillers and additives in various manufacturing products and materials including insulation materials. Alternative to provide eco-friendly and sustainable sources of nanocellulose from various resources has gained significant interest from both academia and industries. CNC filler offers a lower production cost, which is below 10 USD/kg [27] compared to other nanofillers, such as chitosan (15 USD/kg) [28] or inorganic nanoparticles including ZnO (840 USD/kg), Al_2O_3 (960 USD/kg), and TiO_2 (1543 USD/kg) nanoparticles [29]. Considering the significance of CNC over other nanofillers, herein, this research aimed to investigate the structure-properties relationship of RPUF composites by tuning CNC from OPEFB in RPUF regarding physio-chemical performances and insulation properties. Further, most studies have reported the properties of RPUF such as thermal conductivities and mechanical properties, without further impact analysis of the RPUF composite used as a thermal insulation on energy efficiency and GHG reduction. To the best of our knowledge, there are no studies that reported comprehensive analysis and calculation to determine the benefit of RPUF reinforcement CNC derived from OPEFB in energy efficiency and its environmental impact on GHG emission. Therefore, the potential of RPUF-CNC composites derived from OPEFB as thermal insulators to improve energy efficiency and CO_2 reduction was also comprehensively studied to offer robust solutions in combating energy and environmental crises using sustainable materials.

2 Materials and Methods

2.1 *Materials*

PT Mandiri Palmera Agrindo, Luwu, Sulawesi, Indonesia, generously gave oil palm empty fruit bunches (OPEFB). Technical grade NaOH, H_2O_2, and H_2SO_4 were bought from PT. Mahkota Jaya Raya. Polymeric methylene diphenyl diisocyanate (Part A) and polyol blend (Part B) were purchased from PT Justus Kimia Raya.

2.2 *Preparation of Cellulose Nanocrystals (CNC)*

The extraction process of microfiber cellulose (MFC) from OPEFB and further production of CNC was used based on our previous study [30]. MFC is isolated from OPEFB through a pretreatment process through a delignification process using NaOH 10 wt%, then bleached using H_2O_2 4 wt%, 5 grams of obtained MFC was hydrolyzed using 28 wt% of H_2SO_4 at 50 ℃ for 3.5 h followed by centrifugation at 3000 rpm for 5

min. For neutralization purposes, dialysis was conducted for 4–5 days. The CNC solution was then freeze-dried for 4 days to obtain dried CNC.

2.3 *Preparation of RPUF-CNC composites*

Commercially available RPUF blends consist of polyurethane part B (polyol blend) and polyurethane part A (isocyanate) were combined in a 3:2 ratio to produce control RPUF (F_0). A digital overhead stirrer running at 500 rpm for 15 s was used to mix the ingredients. RPUF composite formulations were produced by mixing CNC at various concentrations (0.25 wt%–1 wt%) as shown in Table 1. In Part B for 15 seconds followed by mixing with Part A, denoted for example $FC_{0.5,}$ with 0.5 wt% representing the CNC concentration.

Table 1: RPUF composites formulations.

No	Samples	Mass of CNC (wt%)
1	FC_0	0.00
2	$FC_{0.25}$	0.25
3	$FC_{0.5}$	0.50
4	$FC_{0.75}$	0.75
5	FC_1	1.00

2.4 *Characterization of composites*

The foaming behavior of foam composite formation was monitored using a conventional cup test, which measured various parameters, including cream time, gel time, free-rise time, and tack-free time.

The foam composites were analyzed using a Fourier Transform Infrared spectrophotometer (FTIR Nicolet 1S5-Thermo Scientific/ASB 1706545) with a diamond attenuated total reflection (ATR) accessory. The spectra were recorded in the wavenumber range of 400–4000 cm^{-1}.

The compressive strength and Young's modulus were determined using the universal testing machine (Tensilon) at a speed of 2 mm/min and load cell of 10 kN to a maximum of 10% deformation. The specimens were cut into rectangular shapes according to the specifications outlined in ASTM D1621-10 with dimensions 50×50×40 mm. A minimum of five specimens were tested in parallel and perpendicular orientations relative to the foam rise direction.

The density of the foam composites was determined by calculating the ratio of the sample weight to its volume using a precision electronic balance and digital calipers in accordance with ASTM D1622.

The morphology of the foam composites was analyzed using a scanning electron microscope (JEOL JSM IP300) at 20 kV. The statistical analysis of the cell size was conducted on the basis of the SEM image using ImageJ 1.54d software.

The thermal conductivity (λ) of the foam composites was determined using a QTM-500 quick thermal conductivity meter in accordance with ASTM C518-10 and rectangular specimens (100×50×20 mm).

The dimensional stability of foam composites was analyzed by conditioning samples (40×40×5 mm blocks) at 70 ± 2 °C and −79 ± 2 °C in accordance with ASTM D 2126-09. The conditioning period of one, seven, and 14 days was undertaken, with the dimensions of length, width, and thickness measured before and after treatment with digital calipers. The % linear changes were calculated with the following equation.

$$Linear\ Changes\ (\%) = \frac{V_2 - V_1}{V_1}\ x\ 100\% \quad (1)$$

where,
V_1 = The dimensions before conditioning (mm)
V_2 = The dimensions after conditioning (mm)

The energy efficiency study was carried out based on the obtained thermal conductivity value. Calculations were carried out assuming the basis of room area at 24 m^2 (length of 4 m, width of 2 m, and height of 3 m). The air conditioning (AC) was assumed to be used for 8 hours per day. In this work, it is assumed that the wall with insulation has an outer and inner composition of concrete. Hence, the calculation of the total thermal resistance is summarized in Table 2. Additionally, to calculate the energy cost, the electricity cost is assumed at a price of 0.08 USD/kWh. The energy consumption was calculated using the equation below.

$$Energy\ (Wh) = U\ \times\ A\ \times\ \Delta T\ \times\ t \quad (2)$$

$$U = \frac{1}{R_{total}} \quad (3)$$

$$R = \frac{m}{\lambda} \quad (4)$$

where,
U = Thermal transmittance (W/m^2K)
R = Thermal resistance (m^2K)/W)
λ = Thermal conductivity (W/mK)

m = Thickness of insulation (m)
A = Building areas (24 m^2)
ΔT = Temperature changes (5 °C)
t = Time to use AC (8 h)

Greenhouse gas (GHG) emissions were calculated based on the comparison between the quantity of CO_2 release of the obtained RPUF composites and conventionally used wall material made of wood and concrete respectively. The carbon dioxide (CO_2) gas emissions were calculated using the equation below.

$$CO_2\ quantity = E\ x\ EF \quad (5)$$

where,
E = Energy consumption (kWh/m^2)
EF = Emission factor (0.39 kg CO_2/kWh)

Table 2: Wall structure.

Materials	Thickness Wall (m)			R_{total}
	Internal	Insulation	External	
Without Insulation				
Concrete	0.050	-	0.050	0.05
Wood	0.050	-	0.050	0.77
With Insulation				
RPUF-CNC	0.025	0.050	0.025	1.54
F_0	0.025	0.050	0.025	1.74
$F_{0.5}$	0.025	0.050	0.025	1.88

3 Results and Discussion

3.1 *Foaming behavior of composites*

The foaming behavior of the foam composites requires numerous phases, each monitored simultaneously (Figure 1). The foaming behavior is influenced by various factors, including the type and concentration of fillers, processing conditions, and formulation of the polyurethane. Understanding foaming behavior can optimize the processing condition leading to the production of high-quality RPUF-CNC composites with consistent properties. The foaming behavior parameters of rigid polyurethane foam (RPUF) composites include cream time, gel time, free-rise time, and tack-free time. They are also used to determine the processing conditions including stirring, pouring, and curing times [31]. The cream time is the first phase that occurs when part A and part B are mixed, and gas bubbles begin to develop. A longer cream time can result in a higher density and smaller cell size, which can improve the thermal insulation and mechanical properties of the composite. However, excessively longer cream time can lead to over-foaming, resulting in a lower density influence on reduced thermal and mechanical properties [32]. The gel time, which is the time required for the foam to reach its gel point, is critical in determining the final microstructure and properties of the RPUF-CNC composites. Increasing of gelling time can result in smaller cell size and improved thermal properties [33]. The free-rise time represents the time of the optimal expansion of the foam. The tack-free time can be considered to be the point at which the surface of the foam has dried out and no longer retains any stickiness, hence indicating that the foam has completely cured [34]. In general, gelling time can influence free-rise time and tack-free time as it relates to the formation of nucleation sites for bubble formation [32]. Table 3. shows the time of foaming behavior of the RPUF composites.

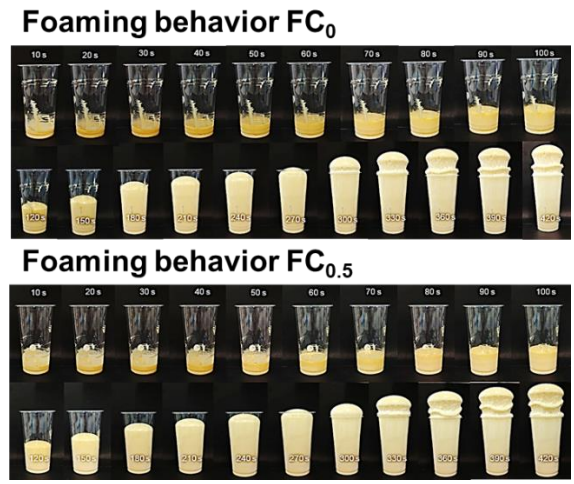

Figure 1: shows the foaming behavior of RPUF-CNC composites.

Table 3: Foaming behavior of RPUF composites.

Samples	Cream Time (s)	Gel Time (s)	Free-rise Time (s)	Tack free Time (s)
F_0	38.52 ± 0.12	219.67 ± 0.79	411.42 ± 2.55	721.00 ± 1.11
$FC_{0,25}$	39.48 ± 0.06	216.53 ± 0.88	412.29 ± 5.81	734.05 ± 0.91
$FC_{0,5}$	39.49 ± 0.70	218.69 ± 2.39	414.18 ± 5.18	737.80 ± 3.33
$FC_{0,75}$	40.57 ± 0.58	222.22 ± 0.02	425.78 ± 2.32	732.36 ± 3.13
FC_1	41.15 ± 1.00	226.70 ± 3.36	430.69 ± 1.83	738.88 ± 2.31

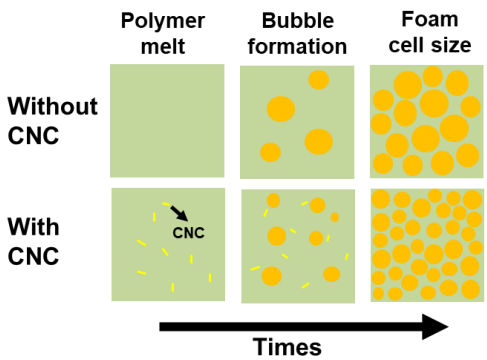

Figure 2: Effect of CNC as a nucleation agent in bubble formation.

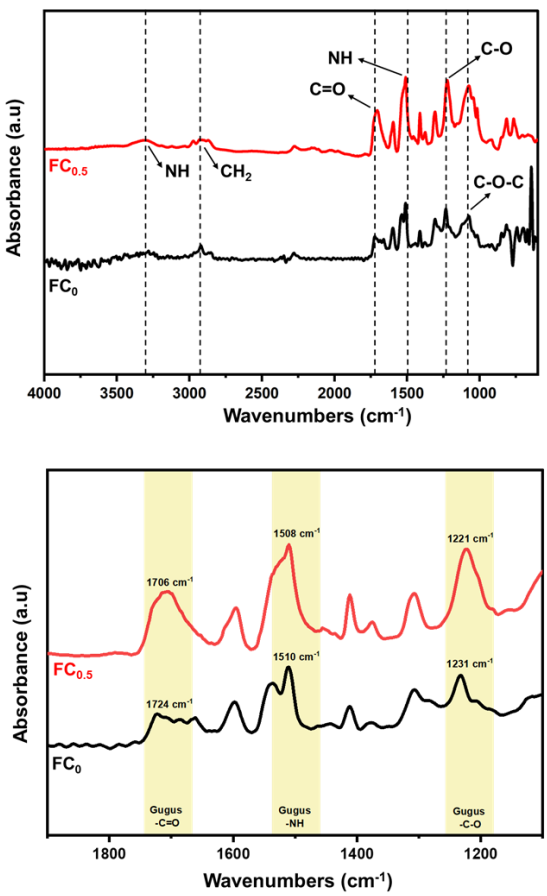

Figure 3: FTIR spectra of RPUF-CNC composites.

The outcomes of the study indicated that the addition of CNC increases the foam formation time. This result is largely related to CNC as a nucleating agent. The increase in reinforcement content affects the reaction kinetics and phase separation. The polymerization rate of PU during foam formation and cellular structure development becomes slower compared to the control RPUF (FC_0) without any CNC. The addition of fillers to the system decreases the isocyanate conversion rate during the initial stages of the reaction. Additionally, the presence of fillers causes a decline in molecular mobility, leading to longer cream time and tack-free time [35].

The foaming mechanism upon the addition of CNC to RPUF highly affects the creation of nucleation sites during bubble formation as depicted in Figure 2. The mechanism underlying nucleation to cell size involves the rate of nucleation site formation and subsequent cell growth from these sites. When the nucleation rate is high, a large number of small nuclei are formed, and each of them is developed into a small cell due to limited resources and space for growth. Conversely, when the nucleation rate is low, a smaller number of nuclei are formed, allowing each nucleus to grow larger as it has more resources and space available. The interaction between the nucleation rate and the availability of resources for cell growth determines the final size and distribution of the cells. In addition, the presence of CNC is expected to result in the formation of the intermolecular network between CNC and polyurethane, as well as intramolecular hydrogen bonding among CNCs. This results in a longer foaming time (Table 3) and reduces the cell size and thus the increase in solid polymeric network packing density of the RPUF, leading to the improvement in the mechanical properties [32]. The effect of CNC incorporation on the morphological structure of RPUF composite is discussed further in the following discussion.

3.2 *Fourier transform infrared (FTIR) of composites*

The FTIR analysis was used to identify the functional group of the foam composites, as reported in Figure 3. The vibration band at wavenumber 3288 cm^{-1} corresponds to the stretching of the aliphatic primary amine functional group (N-H). The asymmetric vibration band at wavenumber 2930 cm^{-1} is characteristic of aliphatic CH_2 [36]. In comparison to other studies that identified NH stretching groups at wavenumbers 3310 cm^{-1} [37] and 3336 cm^{-1} [38], this peak is typically observed within the range of 3300–3400 cm^{-1}. Its presence is indicative of the presence of urethane linkage in polyurethane. Moreover, the wavenumber of 1720 cm^{-1} is characteristic of the carbonyl group (C=O) of isocyanate and polyurethane. The chemical linkage of C=O and C-O-C is

representative of the urethane bond in the gelling reaction. The vibration band at 1510 cm^{-1} indicates the bending of the N-H groups in polyurethane, while a wavenumber of 1235 cm^{-1} indicates C-O-C stretching. The blowing reaction is a reaction between the amine and carbonyl group resulting in CO_2. Finally, the wavenumber 1079 cm^{-1} corresponds to the stretch of the C-O bond.

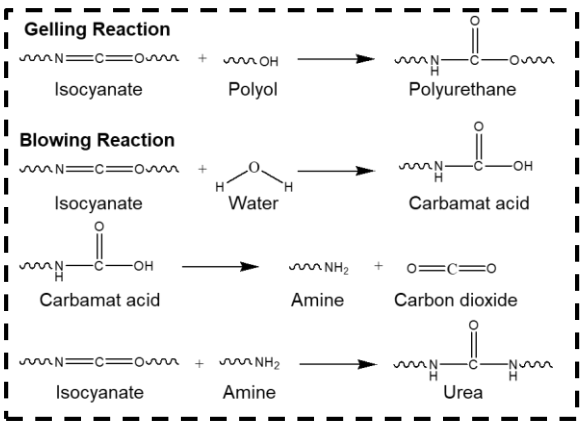

Figure 4: Reaction during polyurethane formation.

The formation of RPUF involves two main reactions, namely the gelling reaction and the blowing reaction, and is explained in Figure 4. During the gelling reaction, isocyanate reacts with a polyol to produce urethane bonds, which increase the molecular weight of the polymer. In contrast, during the blowing reaction, isocyanate reacts with air to produce amines and carbon dioxide. Subsequently, amines undergo a chemical reaction with isocyanates, resulting in the formation of urea linkages and the release of carbon dioxide. This process leads to the development of foam and the expansion of the material, providing a cellular structure [39].

In general, the presence of hydrogen bonds upon adding nanofiller such as CNC in the polymer matrix could be observed by the shifting of the vibration or the peak position in the FTIR analysis. The higher the number of hydrogen bonds formed, the greater the possibility of shifting the peaks depending on the interaction and surrounding groups [40], [41]. Figure 3 shows that there are two shifting vibrations observed in the FTIR spectrum of wavenumbers 1800–1200 cm^{-1} normalized to absorption. First, the carbonyl group (C=O) at wavenumbers of 1724 cm^{-1} to 1706 cm^{-1} for control RPUF (FC_0) and RPUF-CNC composite ($FC_{0.5}$), respectively. Secondly, there is also the shifting of N-H bending from 1508 cm^{-1} to 1510 cm^{-1} indicating the existence of a hydrogen bond interaction between the H atom on the amine group of polyurethane and the O atom on the OH group of CNC. In agreement with other studies, the addition of CNC which is rich in hydroxyl groups in polyurethane matrix has been reported to induce a shifting peak of surrounding groups closed by the hydrogen bonds interaction at 1707, 1600, and 1528 cm^{-1} corresponding to C=O, C=C, and N-H functional groups (as depicted in Figure 5) in urethane bonds [37].

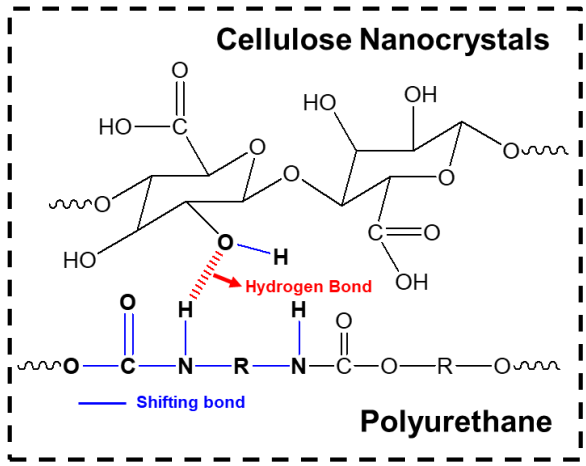

Figure 5: Hydrogen bond interaction between polyurethane and CNC.

3.3 *Surface morphology analysis of composites*

The structure of composite foam is typically polygonal consisting of dominant closed cells. A recent study revealed that the addition of more CNC mass leads to a reduction in cell size. There is a noticeable difference in cell size both parallel or perpendicular to the foam rise between RPUF control without any CNC and RPUF composite with CNC inclusion. The decrease in cell size is caused by one of the CNCs acting as a nucleating agent and controlling bubbles from merging [25].

The sizes of control RPUF and RPUF-CNC composites are displayed using a Scanning Electron Microscope (SEM) analysis in Figure 6. The perpendicular pore size is lower than the parallel from the rise. This difference is simply due to a common phenomenon in polyurethane foam during foam formation and processing. During the foaming process, the foam rises through the cells are formed by the expansion of the gas bubbles parallel to the foam rise, which leads to larger and more variable cell sizes. As discussed previously in the kinetic study, the

presence of CNC in RPUF functions as a nucleating agent, that increases the number of cell formation starting points during the polyurethane (PU) foaming process. This increases the number of cells and a reduction in the average cell size (Figure 2). This reduced cell size, consequently increases in packing density leading to the higher density of the foam, which can improve its mechanical properties. The change in morphological structure, as noted by the reduced size of the RPUF foam cell upon the addition of CNC, significantly affects the performance of RPUF, which is further discussed in the following section. The addition of 0.5 wt% CNC ($FC_{0.5}$) decreased cell size from 818 to 761 µm (6.97%, by parallel foam rise) and from 792 to 569 µm (28.16%, by perpendicular foam rise). This is related to the interconnections in the cellular structure, which causes a smaller cell-size foam with the addition of CNC [42]. Additionally, the distribution of struts through the foam could affect the thermal insulation properties. The struts reduce the rate of gas diffusion, resulting in a decrease in thermal conductivity [6]. The cell size distribution of the RPUF-CNC composite is shown in Figure 7. The cell size distribution in the perpendicular RPUF is more homogeneous than in the parallel RPUF. This is attributed to a more homogeneous nucleation and growth process. This homogeneity is likely to improve the thermal insulation properties of the foam, as a more homogeneous cell size traps gas more effectively and reduces thermal conductivity.

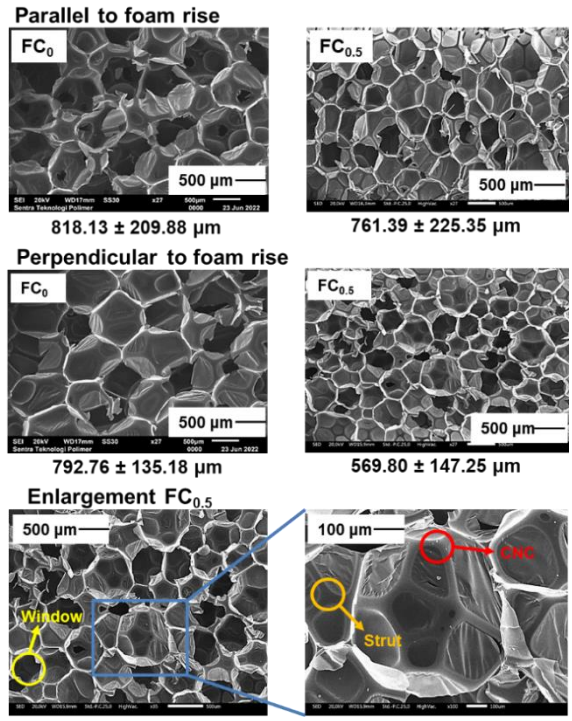

Figure 6: SEM image of the surface area of RPUF without and with CNC in the direction parallel to the foam rise (↑rise).

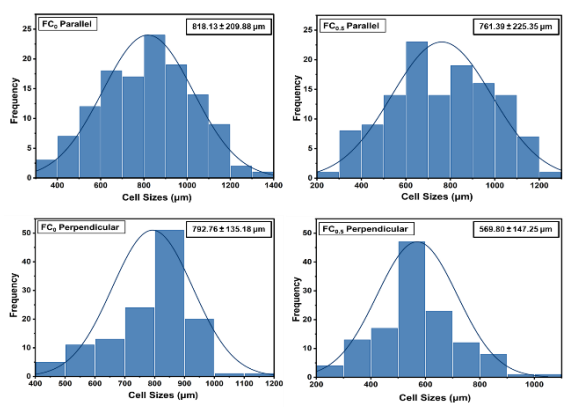

Figure 7: Distribution of cell sizes of RPUF-CNC composite.

3.4 *Mechanical properties of composites*

The density of foam is largely affected by its structure, as the higher density is attributed to a denser structure. The compressive strength of foam is also heavily influenced by its density, which is related to the bonds formed and the morphological structure of the foam. According to the results obtained, the resulting composite has a density of around 37–39 kg/m^3, which is in line with the typical thermal insulation specifications for buildings between 30–40 kg/m^3. The addition of low loading of CNC did not provide a significant change in density.

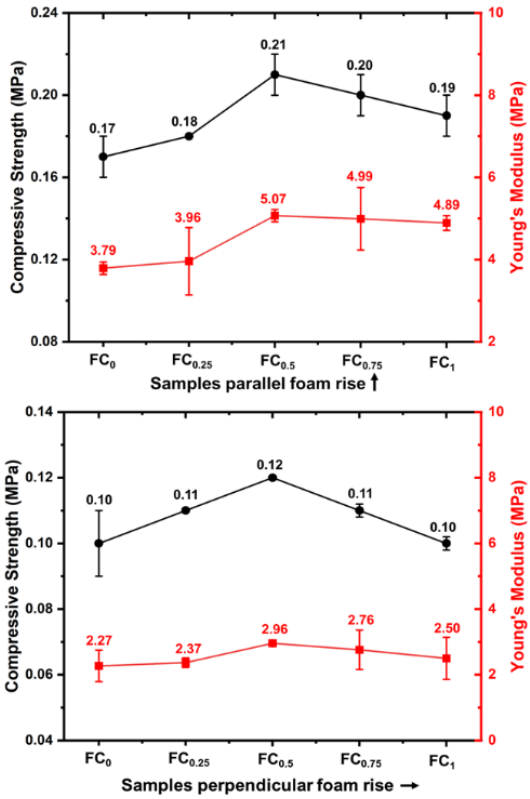

Figure 8: Mechanical properties of RPUF-CNC composite.

The compressive strength and Young's modulus of the RPUF reinforcement CNC from OPEFB composites are summarized in Figure 8. The results showed that the compressive strength for parallel to foam rise of control RPUF without nanofillers increased by 23.53% from 0.17 MPa to 0.21 MPa upon the incorporation of 0.5 wt% of CNC. In addition, the improvement of compressive strength for perpendicular foam rise was also observed by 20% from 0.10 MPa to 0.12 MPa. Furthermore, there are significant improvements in Young's modulus by 33.77% and 30.39% for parallel foam rise and perpendicular foam rise, respectively. These are due to the smaller cell sizes, which increase the packing network interconnection [17]. Compared to other research, for example, CNC from algae can increase the compressive strength of RPUF by 4.52% [23]. Meanwhile, the CNC from cotton has been reported to significantly improve the RPUF by 1.2% [25]. In this work, the enhancement in mechanical properties upon the incorporation of CNC from OPEFB in RPUF is significantly greater than that of RPUF reinforced with CNC derived from algae and cotton.

3.5 *Thermal insulation properties of composites*

The thermal insulation properties are characterized by the thermal conductivity value. The thermal conductivity analysis determines how well a material can transfer heat from one place to another. This is significant when considering its function as thermal insulation. The smaller the thermal conductivity value of a material, the better it can serve as thermal insulation. The thermal conductivity coefficient is one of the basic parameters of RPUF. The thermal insulation materials currently available on the commercial market have a coefficient of thermal conductivity of between 0.02 and 0.04 W/(m·K) coefficient. Thermal conductivity is a complex property that is influenced by multiple factors. The primary contributors to this property can be broadly classified into three categories: conduction through the polymer phase, conductivity through gases that have been trapped in closed cell structures, and intercellular radiation [33]. First, conduction through the polymer phase is influenced by chain structure and polymer matrix. The chain structure includes crystallinity, orientation, and crosslinking density. Crystalline regions have higher thermal conductivity due to the ordered molecular structure, whereas amorphous regions have lower conductivity due to the disordered molecular structure. Second, conductivity through gases that have been trapped in closed cell structures can significantly enhance thermal conductivity because gases have a higher thermal conductivity than the polymer. Third, inter-cellular radiation or thermal radiation leads the heat transfer.

For the case of the conductivity through gas that has been trapped in a closed cell structure, it does not have a significant effect in this work because the same blowing agent was used for all formulations. In this work, the addition of CNC affects the thermal conductivity based on the conduction through the polymer phase and thermal radiation. Conduction through the polymer phase occurs in connection with the addition of CNC as a nucleation agent which can increase the initial amount of nucleation in foam formation so that the cell size becomes smaller (Figure 2). In the case of thermal radiation, the influencing factor is the cell dimensions. Radiation is the transfer of heat by electromagnetic waves, such as infrared light. These waves can travel through both air and struts. When the cell size is reduced and the number of supports is increased, the radiation transmitted through the struts is limited.

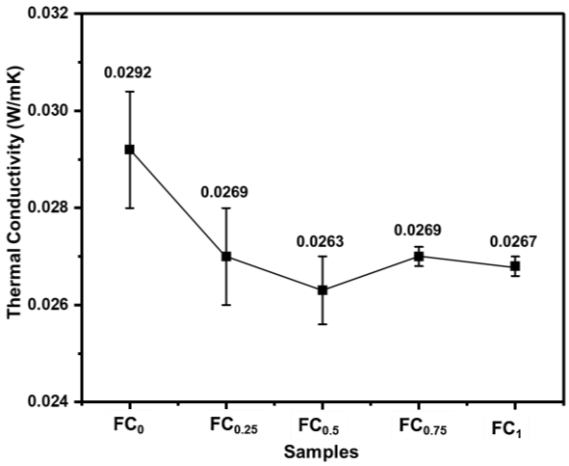

Figure 9: Thermal conductivity of RPUF-CNC composites.

Figure 9 presents the thermal conductivity values of the RPUF composite at different concentrations upon CNC addition at varied concentrations. The optimum properties of RPUF composite are obtained with the addition of 0.5% CNC, at a conductivity value of 0.0263 W/mK equal to improve the thermal insulation property by 9.95% compared to foam composite control, which is relatively higher than other studies of RPUF composite reinforced with CNC from microcrystal cellulose by 0.0333w/mK insulation performance [22] and from CNC commercial at 0.0441 W/mK insulation performance [43]. In addition, the use of nanographene at 0.3% as a filler in RPUF has been reported to reduce the conductivity by 2.1% compared to the control [44]. As discussed previously, this is because smaller cells lower the amount of heat that can be transported through the foam by conduction and radiation, resulting in improved thermal insulation. The presence of CNC on the strut [Figure 6] increases the length of the heat transfer path and decreases the radiative conductivity. Moreover, the homogeneous and smaller cells reduce the thermal conductivity by limiting the heat transfer path through the gas phase and solid phase of the foam.

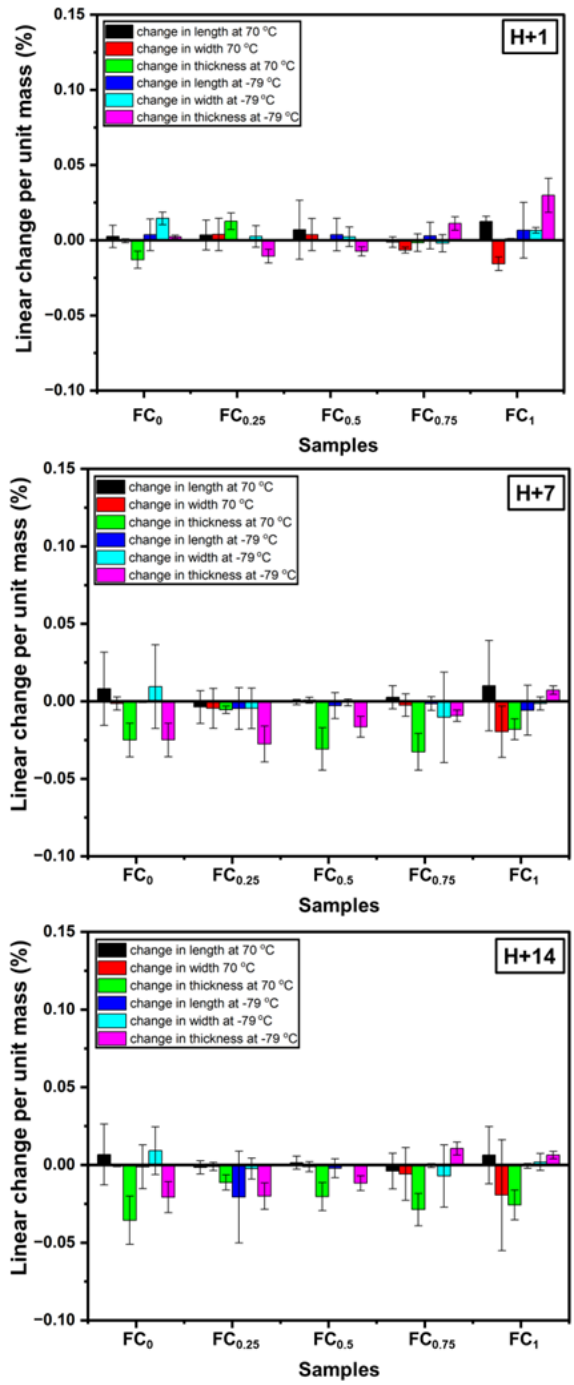

Figure 10: The percentage linear change per unit of mass at temperatures of 70 ± 2 °C and −79 ± 2 °C following exposure.

3.6 *Dimensional stability*

The dimensional stability was determined based on linear length, width, and thickness changes. The analysis of dimensional stability is of significant importance for the properties of polyurethanes in the context of building material standards that can be functionally used in both extremely low and high temperatures. The data imply their durability of practical use when the RPUF is applied at extreme temperatures. We provide the industrial requirements based on BS4370: Part 1: 1988 for building panels showed that the linear changes of building panels tested under extreme temperature over 24 h, should be fewer than 3% and 1% linear changes at 70 °C and –15 °C, respectively [33]. Figure 10 shows that the results of the dimensional changes under extreme temperature exposure at both −79 ± 2 °C and +70 ± 2 °C are below 3%. This finding is consistent with the results of previous research, that the incorporation of CNC from wood on the RPUF can enhance dimensional stability in comparison to the control sample, which was tested in freezing (–25 °C) and heating (60 °C) conditions [45]. In comparison to other insulation materials such as concrete, wood, brick, and extruded polystyrene foam (EPS), the recommended linear change of this work is also within similar specifications at less than 2% [46].

3.7 *Efficiency energy studies of RPUF composite as thermal insulation material for building*

Implementing thermal insulation in the built environment has been identified as an effective means of achieving energy efficiency and conservation. A suitable selection of appropriate wall insulation materials could result in a reduction in the initial investment and the total energy consumption of the building over its entire life cycle [47]. The calculation of energy efficiency of the obtained RPUF insulation was compared to conventional buildings including concrete and wood material. Table. 4 explains the energy consumption from various wall materials. It resulted that the use of insulation material in building walls can reduce electrical energy. The influence of adding CNC to the RPUF ($FC_{0.5}$) could increase energy saving and efficiency as noted by the reduction of energy consumption from 19.20 kWh and 1.25 kWh by using concrete and wood, respectively into significantly lower of 0.51 kWh by using optimum RPUF-CNC insulating material. In this work, the use of insulating material based on a room area of 24 m^2 can reduce the greenhouse gas (GHG) emissions at 218 kg CO_2 and save up to 284 kWh in comparison to a room without insulation. A comparison with another study that uses wooden PU-CNC composite [22], utilizing OPEFB RPUF-CNC composite as insulation material can reduce energy consumption by 18.24% at 0.12 kWh/room area of 24 m^2 which equals a saving on monthly costs at 0.73 USD. The application of thermal insulation to buildings has been identified as an effective method for achieving cost-effective energy conservation. The selection of appropriate insulation composite materials can result in a significant reduction in energy consumption and monthly electricity costs. Further, the utilization of RPUF-CNC composite as a thermal insulator offers a potential reduction in monthly electricity costs by up to 119 USD in comparison to conventional houses made of concrete walls as shown in Table 4.

Table 4: Energy and cost efficiency study.

Characteristics	Concrete	Wood	PU-CNC	FC_0	$FC_{0.5}$
Density (kg/m^3)	2400	670	336	38	38
Thermal Conductivity (W/mK)	2.000	0.130	0.033	0.029	0.027
Thermal Transmittance (m^2K)/W)	20	1.3	0.86	0.76	0.71
Energy (kWh)	19.20	1.25	0.63	0.55	0.51
Energy (kWh/m^2)	0.8	0.052	0.026	0.023	0.021
Monthly cost (USD)	122.8	7.99	3.99	3.54	3.26
CO_2 gas emissions (kg CO_2/m^2)	0.312	0.021	0.010	0.009	0.008
Reference	[48]	[48]	[22]	This work	This work

3.8 *Greenhouse gas emissions*

A recent estimate suggests that up to 40% of Global Greenhouse Gas (GHG) emissions can be attributed to activities of the Architecture, Engineering, and Construction industry (AEC) industry [49]. The massive amount of required insulated building's fuel usage comes significantly to maintain the desired temperature for comfortable human activity. The right selection of insulation materials might help not only to minimize heat loss through the building envelope but also mitigate gas emissions issues. The combustion of fuel energy produces atmospheric gases (e.g., CO_2, SO_2, CO, H_2O) [50]. The calculation of energy efficiency and its contribution to the reduction of greenhouse gas (GHG) emissions is calculated in the Table 4. The overall analysis shows that RPUF-CNC

composite at optimal formulation $FC_{0.5}$ can contribute to the reduction of GHG at 0.31 and 0.02 kg CO_2/m^2 compared to concrete and wood, respectively. Furthermore, the use of insulating material based on a room area of 24 m^2 can reduce the greenhouse gas (GHG) emissions of 7.3 kg CO_2 in comparison to a room without insulation. In comparison with another study, this present work on RPUF composites containing CNC from OPEFB at 0.5 wt% ($FC_{0.5}$) showed a higher reduction of GHG emissions by 0.002 kg CO_2/m^2 equivalent to 0.05 kg CO_2 based on a room area of 24 m^2 than RPUF reinforced with CNCs derived from wood [22]. Further, the utilization of OPEFB waste into value-added additives in RPUF also drives the reduction of CO_2 emissions related to waste reduction in the environment.

4 Conclusions

RPUF composite foams reinforced with different concentrations of CNC derived from biomass waste of oil palm fruit empty bunches (OPEFB) at various concentrations from 0.25% up to 1% were successfully produced as a promising insulation material to boost the energy efficiency of buildings. The results presented demonstrated that incorporating CNC enhanced the thermal insulation and the mechanical properties. The results demonstrated that incorporating CNC enhanced the thermal insulation and the mechanical properties. It can be concluded from the results that the addition of 0.5 wt% CNC to RPUF composite foams optimally improved the compressive strength by 23.53% and thermal insulation properties by 9.95% compared to neat foam composite without CNC. Based on the study on energy efficiency, RPUF composites at 0.5 wt% CNC resulted in an enhancement of energy efficiency in buildings at up to 0.78 kWh/m^2 and 0.031 kWh/m^2 compared to buildings using concrete and wood, respectively. For the case of GHG reduction, the CNC incorporation in RPUF composite reduced greenhouse gas (GHG) emissions by 110 and 7.2 kg CO_2/year in comparison to conventional walls made of concrete and wood, respectively. For long-term impact, the use of slabs RPUF reinforced from CNC derived from OPEFB, at 24 m^2 could significantly reduce 110 kg CO_2/year/house. As previous report, insulated foam material could be used for up to 50 years, hence the long-term use of RPUF-CNC OPEFB could significantly achieve a reduction of 5.5 ton CO_2, equally saving up 74,752 kWh savings/room at the end of its useful life. Utilizing CNC derived from OPEFB contributes to the improvement and mitigation of environmental concerns. This sustainable approach aligns with green building technologies, promoting the use of environmentally friendly materials, and reducing their long-term environmental impact. Moreover, the application of RPUF-CNC composites as thermal insulation in buildings offers a promising solution in terms of enhancing energy efficiency, reducing energy operational costs, and decreasing greenhouse gas emissions. Further investigations should include the life-cycle assessment and production cost of developed materials (CNC and RPUF-CNC slabs) to provide a comprehensive analysis of the potential use of OPEFB RPUF-CNC and its impact on GHG reduction for scientific recommendation of energy-efficient systems and implementation of sustainable practices.

Acknowledgments

The authors are grateful to acknowledge financial support from Prioritas Nasional Energi Baru Terbarukan OREM-BRIN. Dilla Dayanti gratefully received the scholarship from Degree by Research, the National Research and Innovation Agency (BRIN). The authors are also grateful for the analysis support from E-Layanan Sains (ELSA) BRIN.

Author Contributions

A.A.S.: conceptualization, supervision, resources, writing—review and editing; D.D.: the design process and characterization, formal analysis, writing—original draft, review, and editing; M.C.: supervision, resources, review, and editing; N.F.: writing, methodology, experiment; P.: review and editing, insulation characterization; M.S.: review and editing; H.: review and editing, mechanical characterization; Y.S.R.: editing, and chemical characterization; R.A.I.: review and editing; P.K.A.: review and editing; S.: analysis preparation and technical project assistance. All authors have read and agreed to the published version of the manuscript.

Conflicts of Interest

The authors declare no conflict of interest.

References

[1] M. Farghali, A. I. Osman, I. M. A. Mohamed, Z. Chen, L. Chen, I. Ihara, P.-S. Yap, and D. W.

Rooney, "Strategies to save energy in the context of the energy crisis: A review," *Environmental Chemistry Letters*, vol. 21, no. 4, pp. 2003–2039, 2023. doi: 10.1007/s10311-023-01591-5.

[2] X. Meng, B. Yan, Y. Gao, J. Wang, W. Zhang, and E. Long, "Factors affecting the in situ measurement accuracy of the wall heat transfer coefficient using the heat flow meter method," *Energy and Buildings*, vol. 86, pp. 754–765, Jan. 2015, doi: 10.1016/j.enbuild.2014.11.005.

[3] A. Almusaed, A. Almssad, A. Alasadi, I. Yitmen, and S. Al-Samaraee, "Assessing the role and efficiency of thermal insulation by the 'BIO-GREEN PANEL' in enhancing sustainability in a built environment," *Sustainability (Switzerland)*, vol. 15, p. 25, 2023, doi: 10.3390/su151310418.

[4] G. Tang, L. Zhou, P. Zhang, Z. Han, D. Chen, X. Liu, and Z. Zhou, "Effect of aluminum diethylphosphinate on flame retardant and thermal properties of rigid polyurethane foam composites," *Journal of Thermal Analysis and Calorimetry*, vol. 140, no. 2, pp. 625–636, Apr. 2020, doi: 10.1007/s10973-019-08897-z.

[5] L. He, F. Chu, X. Zhou, L. Song, and Y. Hu, "Cactus-like structure of BP@MoS2 hybrids: An effective mechanical reinforcement and flame retardant additive for waterborne polyurethane," *Polymer Degradation and Stability*, vol. 202, Aug. 2022, Art. no. 110027, doi: 10.1016/j.polymdegradstab.2022.110027.

[6] Y. Tao, P. Li, H. Zhang, S. Q. Shi, J. Zhang, and Q. Yin, "Compression and flexural properties of rigid polyurethane foam composites reinforced with 3D-printed polylactic acid lattice structures," *Composite Structures*, vol. 279, Jan. 2022, Art. no. 114866, doi: 10.1016/j.compstruct.2021.114866.

[7] M. Albozahid, S. A. Habeeb, N. A. I. Alhilo, and A. Saiani, "The impact of graphene nanofiller loading on the morphology and rheology behaviour of highly rigid polyurethane copolymer," *Materials Research Express*, vol. 7, no. 12, Dec. 2020, Art. no. 125304, doi: 10.1088/2053-1591/aba5ce.

[8] S. B. Nagaraju, M. Puttegowda, Y. G. T. Girijappa, N. K. Rawat, A. Verma, S. M. Rangappa, and S. Siengchin, "Mechanical characterization and water absorption behavior of waste coconut leaf stalk fiber reinforced hybrid polymer composite: Impact of chemical treatment," *Applied Science and Engineering Progress*, vol. 17, no. 3, May 2024, doi: 10.14416/j.asep.2024.05.003.

[9] V. Dogra, C. Kishore, A. Verma, A. K. Rana, and A. Gaur, "Fabrication and experimental testing of hybrid composite material having biodegradable bagasse fiber in a modified epoxy resin: evaluation of mechanical and morphological behavior," *Applied Science and Engineering Progress*, vol. 14, no. 4, Jun. 2021, doi: 10.14416/j.asep.2021.06.002.

[10] M. Chanes de Souza, I. Moroz, I. Cesarino, A. L. Leão, M. Jawaid, and O. A. Titton Dias, "A review of natural fibers reinforced composites for railroad applications," *Applied Science and Engineering Progress*, vol. 15, no. 2, Mar. 2022, doi: 10.14416/j.asep.2022.03.001.

[11] M. Stanzione, M. Oliviero, M. Cocca, M. E. Errico, G. Gentile, M. Avella, M. Lavorgna, G. G. Buonocore, and L. Verdolotti, "Tuning of polyurethane foam mechanical and thermal properties using ball-milled cellulose," *Carbohydrate Polymers*, vol. 231, Mar. 2020, Art. no. 115772, doi: 10.1016/j.carbpol.2019.115772.

[12] C. Santos, T. Santos, K. Moreira, M. Aquino, and R. F. Lucas Zillio, "Statistical study of the influence of fiber content, fiber length and critical length in the mechanical behavior of polymeric composites reinforced with carica papaya fibers (CPFs)," *Applied Science and Engineering Progress*, vol. 14, no. 4, Jul. 2021, doi: 10.14416/j.asep.2021.07.002.

[13] A. Dhandapani, S. Krishnasamy, T. Ungtrakul, S. M. K. Thiagamani, R. Nagarajan, C. Muthukumar, and G. Chinnachamy, "Desirability of tribo-performance of natural based thermoset and thermoplastic composites: A concise review," *Applied Science and Engineering Progress*, vol. 14, no. 4, Jul. 2021, doi: 10.14416/j.asep.2021.07.001.

[14] N. A. Azra, A. Atiqah, H. Fadhlina, M. A. Bakar, A. Jalar, R. A. Ilyas, J. Naveen, F. A. Sabaruddin, K. K. Lim, and M. Asrofi, "Oil-palm based nanocellulose reinforced thermoplastic polyurethane for plastic encapsulation of biomedical sensor devices: water absorption, thickness swelling and density properties," *Applied Science and Engineering Progress*, vol. 16, no. 1, Feb. 2022, doi: 10.14416/j.asep.2022.02.001.

[15] R. Gu, M. M. Sain, and S. K. Konar, "A feasibility study of polyurethane composite foam

with added hardwood pulp," *Industrial Crops and Products*, vol. 42, pp. 273–279, Mar. 2013, doi: 10.1016/j.indcrop.2012.06.006.

[16] S. Ju, A. Lee, Y. Shin, H. Jang, J.W. Yi, Y. Oh, N.J. Jo, and T. Park, "Preventing the collapse behavior of polyurethane foams with the addition of cellulose nanofiber," *Polymers*, vol. 15, no. 6, 2023, doi: 10.3390/polym15061499.

[17] C. L. Yiin, S. Ho, S. Yusup, A. T. Quitain, Y. H. Chan, A. C. M. Loy, and Y. L. Gwee, "Recovery of cellulose fibers from oil palm empty fruit bunch for pulp and paper using green delignification approach," *Bioresource Technology*, vol. 290, Oct. 2019, Art. no. 121797, doi: 10.1016/J.BIORTECH.2019.121797.

[18] F. Jiang and Y.-L. Hsieh, "Super water absorbing and shape memory nanocellulose aerogels from TEMPO-oxidized cellulose nanofibrils via cyclic freezing–thawing," *Journal of Materials Chemistry A*, vol. 2, no. 2, pp. 350–359, 2014, doi: 10.1039/C3TA13629A.

[19] S. K. Evans, O. N. Wesley, O. Nathan, and M. J. Moloto, "Chemically purified cellulose and its nanocrystals from sugarcane baggase: isolation and characterization," *Heliyon*, vol. 5, no. 10, Oct. 2019, Art. no. e02635, doi: 10.1016/j.heliyon.2019.e02635.

[20] B. S. L. Brito, F. V. Pereira, J.-L. Putaux, and B. Jean, "Preparation, morphology and structure of cellulose nanocrystals from bamboo fibers," *Cellulose*, vol. 19, no. 5, pp. 1527–1536, Oct. 2012, doi: 10.1007/s10570-012-9738-9.

[21] D. Zheng, Y. Zhang, Y. Guo, and J. Yue, "Isolation and characterization of nanocellulose with a novel shape from walnut (*Juglans regia* l.) shell agricultural waste," *Polymers*, vol. 11, no. 7, p. 1130, Jul. 2019, doi: 10.3390/polym11071130.

[22] V. H. Tran, J.-D. Kim, J.-H. Kim, S.-K. Kim, and J.-M. Lee, "Influence of cellulose nanocrystal on the cryogenic mechanical behavior and thermal conductivity of polyurethane composite," *Journal of Polymers and Environment*, vol. 28, no. 4, pp. 1169–1179, Apr. 2020, doi: 10.1007/s10924-020-01673-3.

[23] V. Jonjaroen, S. Ummartyotin, and S. Chittapun, "Algal cellulose as a reinforcement in rigid polyurethane foam," *Algal Research*, vol. 51, Oct. 2020, Art. no. 102057, doi: 10.1016/j.algal. 2020.102057.

[24] A. Redondo, N. Mortensen, K. Djeghdi, D. Jang, R. D. Ortuso, C. Weder, L. T. J. Korley, U. Steiner, and I. Gunkel "Comparing percolation and alignment of cellulose nanocrystals for the reinforcement of polyurethane nanocomposites," *ACS Applied Materials and Interfaces Journal*, vol. 14, no. 5, pp. 7270–7282, Feb. 2022, doi: 10.1021/acsami.1c21656.

[25] A. A. Septevani, P. K. Annamalai, and D. J. Martin, "Synthesis and characterization of cellulose nanocrystals as reinforcing agent in solely palm based polyurethane foam," *AIP Conference Proceedings*, vol. 1904, no. 1, Nov. 2017, doi: 10.1063/1.5011899.

[26] A. A. Septevani, D. A. C. Evans, P. K. Annamalai, and D. J. Martin, "The use of cellulose nanocrystals to enhance the thermal insulation properties and sustainability of rigid polyurethane foam," *Industrial Crops and Products*, vol. 107, pp. 114–121, 2017, doi: 10.1016/j.indcrop.2017.05.039.

[27] N. D. Sanandiya, Y. Vijay, M. Dimopoulou, S. Dritsas, and J. G. Fernandez, "Large-scale additive manufacturing with bioinspired cellulosic materials," *Nature*, vol. 8, no. 1, p. 8642, Jun. 2018, doi: 10.1038/s41598-018-26985-2.

[28] J. Weng, A. Durand, and S. Desobry, "Chitosan-based particulate carriers: Structure, production, and corresponding controlled release," *Pharmaceutics*, vol. 15, no. 5, p. 1455, May 2023, doi: 10.3390/pharmaceutics15051455.

[29] T. Elango, A. Kannan, and K. Kalidasa Murugavel, "Performance study on single basin single slope solar still with different water nanofluids," *Desalination*, vol. 360, pp. 45–51, Mar. 2015, doi: 10.1016/j.desal.2015.01.004.

[30] F. Yurid, A. S. Handayani, F. D. Maturbongs, Y Irawan4, Y. Sampora, Y A Devy, M Septiyanti, D. Ramdani, E. Supriadi, and K. N. M. Amin "Production of nanocellulose using controlled acid hydrolysis from large-scale production of micro-fibrillated cellulose derived from oil palm empty fruit bunches," *in IOP Conference Series: Earth and Environmental Science*, vol. 1201, no. 1, 2023, Art. no. 012078, doi: 10.1088/1755-1315/1201/1/012078.

[31] M. V. Gangoiti and P. J. Peruzzo, "Cellulose nanocrystal reinforced acylglycerol-based polyurethane foams," *Express Polymer Letters*, vol. 14, no. 7, pp. 638–650, 2020, doi: 10.3144/expresspolymlett.2020.52.

[32] O. F. Olanrewaju, I. O. Oladele, T. F. Omotosho, F. A. Atilola, and S. O. Adelani, "Influence of quartz and marble on the performance of

particulate-filled rigid polyurethane foams," *Journal of Engineering and Technology*, vol. 6, no. 1, pp. 008–025, Feb. 2024, doi: 10.53022/oarjet.2024.6.1.0011.

[33] A. A. Septevani, D. A. C. Evans, C. Chaleat, D. J. Martin, and P. K. Annamalai, "A systematic study substituting polyether polyol with palm kernel oil based polyester polyol in rigid polyurethane foam," *Industrial Crops and Products*, vol. 66, pp. 16–26, Feb. 2015, doi: 10.1016/j.indcrop.2014.11.053.

[34] T. Kattiyaboot and C. Thongpin, "Effect of natural oil based polyols on the properties of flexible polyurethane foams blown by distilled water," *Energy Procedia*, vol. 89, pp. 177–185, Jun. 2016, doi: 10.1016/j.egypro.2016.05.024.

[35] A. Strąkowska, S. Członka, and K. Strzelec, "POSS compounds as modifiers for rigid polyurethane foams (composites)," *Polymers*, vol. 11, no. 7, p. 1092, Jun. 2019, doi: 10.3390/polym11071092.

[36] A. A. Septevani, D. A. C. Evans, D. J. Martin, P. Song, and P. K. Annamalai, "Tuning the microstructure of polyurethane foam using nanocellulose for improved thermal insulation properties through an efficient dispersion methodology," *Polymer Composites*, vol. 44, no. 12, pp. 8857–8869, Sep. 2023, doi: 10.1002/pc.27743.

[37] L. D. Mora-Murillo, F. Orozco-Gutierrez, J. Vega-Baudrit, and R. J. González-Paz, "Thermal-mechanical characterization of polyurethane rigid foams: Effect of modifying bio-polyol content in isocyanate prepolymers," *Journal Renewable Materials*, vol. 5, no. 3, pp. 220–230, Jul. 2017, doi: 10.7569/JRM.2017.634112.

[38] T. Boulaouche, D. E. Kherroub, K. Khimeche, and M. Belbachir, "Green strategy for the synthesis of polyurethane by a heterogeneous catalyst based on activated clay," *Research on Chemical Intermediates*, vol. 45, no. 6, pp. 3585–3600, Jun. 2019, doi: 10.1007/s11164-019-03810-7.

[39] A. Ivdre, A. Abolins, N. Volkovs, L. Vevere, A. Paze, R. Makars, D. Godina, and J. Rizikovs "Rigid polyurethane foams as thermal insulation material from novel suberinic acid-based polyols," *Polymers*, vol. 15, no. 14, Jul. 2023, doi: 10.3390/polym15143124.

[40] M. Lonescu, *Chemistry and Technology of Polyols for Polyurethanes*. 2nd ed. UK: Smithers Rapra Publishing, 2005.

[41] E. Robles, J. Fernández-Rodríguez, A. M. Barbosa, O. Gordobil, N. L. V. Carreño, and J. Labidi, "Production of cellulose nanoparticles from blue agave waste treated with environmentally friendly processes," *Carbohydr Polym*, vol. 183, pp. 294–302, Mar. 2018, doi: 10.1016/j.carbpol.2018.01.015.

[42] F. Coccia, L. Gryshchuk, P. Moimare, F. L. Bossa, C. Santillo, E. Barak-Kulbak, L. Verdolotti, L. Boggioni, and G. C. Lama "Chemically functionalized cellulose nanocrystals as reactive filler in bio-based polyurethane foams," *Polymers*, vol. 13, no. 15, p. 2556, Jul. 2021, doi: 10.3390/polym13152556.

[43] S. Anam, H. Kyungrok, K. Taekyeong, J. Jin, and C. I. Woo, "Enhancing thermal and mechanical properties of rigid polyurethane foam with eco-friendly silane-modified cellulose nanocrystals," *Social Science Research Network Journals*, pp. 1–33, Jan. 2024, doi: 10.2139/ssrn.4699987.

[44] A. Lorenzetti, M. Roso, A. Bruschetta, C. Boaretti, and M. Modesti, "Polyurethane-graphene nanocomposite foams with enhanced thermal insulating properties," *Polymers for Advanced Technologies*, vol. 27, no. 3, pp. 303–307, Mar. 2016, doi: 10.1002/pat.3635.

[45] X. Zhou, M. M. Sain, and K. Oksman, "Semi-rigid biopolyurethane foams based on palm-oil polyol and reinforced with cellulose nanocrystals," *Compos Part A: Applied Science and Manufacturing*, vol. 83, pp. 56–62, Apr. 2016, doi: 10.1016/j.compositesa.2015.06.008.

[46] Rockwool, "Dimensional Stability of Rigid Board Insulation Products," 2023. [Online]. Available: https://www.rockwool.com

[47] K. Moncef, *Optimal Design and Retrofit of Energy Efficient Buildings, Communities, and Urban Centers*. Oxford, UK: Butterworth-Heinemann, 2018.

[48] S. Ilomets, K. Kuusk, L. Paap, E. Arumagi, and T. Kalamees, "Impact of linear thermal bridges on thermal transmittance of renovated apartment buildings," *Journal Of Civil Engineering and Management*, vol. 23, no. 1, pp. 96–104, Jun. 2016, doi: 10.3846/13923730.2014.976259.

[49] M. Płoszaj-Mazurek, E. Ryńska, and M. Grochulska-Salak, "Methods to optimize carbon footprint of buildings in regenerative architectural design with the use of machine learning, convolutional neural network, and

parametric design," *Energies*, vol. 13, no. 20, p. 5289, Oct. 2020, doi: 10.3390/en13205289.

[50] Y. He, T. Kvan, M. Liu, and B. Li, "How green building rating systems affect designing green," *Building and Environment*, vol. 133, pp. 19–31, Apr. 2018, doi: 10.1016/j.buildenv.2018.02.007.